Designation: E 496 – 02

Standard Test Method for Measuring Neutron Fluence and Average Energy from $^{3}H(d,n)^{4}He$ Neutron Generators by Radioactivation Techniques[1]

This standard is issued under the fixed designation E 496; the number immediately following the designation indicates the year of original adoption or, in the case of revision, the year of last revision. A number in parentheses indicates the year of last reapproval. A superscript epsilon (ε) indicates an editorial change since the last revision or reapproval.

1. Scope

1.1 This test method covers a general procedure for the measurement of the fast-neutron fluence rate produced by neutron generators utilizing the $^{3}H(d,n)^{4}He$ reaction. Neutrons so produced are usually referred to as 14-MeV neutrons, but range in energy depending on a number of factors. This test method does not adequately cover fusion sources where the velocity of the plasma may be an important consideration.

1.2 This test method uses threshold activation reactions to determine the average energy of the neutrons and the neutron fluence at that energy. At least three activities, chosen from an appropriate set of dosimetry reactions, are required to characterize the average energy and fluence. The required activities are typically measured by gamma ray spectroscopy.

1.3 *This standard does not purport to address all of the safety concerns, if any, associated with its use. It is the responsibility of the user of this standard to establish appropriate safety and health practices and determine the applicability of regulatory limitations prior to use.*

2. Referenced Documents

2.1 *ASTM Standards:*

E 170 Terminology Relating to Radiation Measurements and Dosimetry[2]

E 181 Test Methods for Detector Calibration and Analysis of Radionuclides[2]

E 261 Practice for Determining Neutron Fluence Rates, Fluence, and Spectra by Radioactivation Techniques[2]

E 265 Test Method for Measuring Reaction Rates and Fast-Neutron Fluences by Radioactivation of Sulfur-32[2]

E 720 Guide for Selection and Use of Neutron-Activation Foils for Determining Neutron Spectra Employed in Radiation-Hardness Testing of Electronics[2]

2.2 *International Commission on Radiation Units and Measurements (ICRU) Reports:*

ICRU Report 13—Neutron Fluence, Neutron Spectra and Kerma[3]

ICRU Report 26—Neutron Dosimetry for Biology and Medicine[3]

2.3 *ISO Standard:*

Guide to the Expression of Uncertainty in Measurement[4]

2.4 *NIST Document:*

Technical Note 1297—Guidelines for Evaluating and Expressing the Uncertainty of NIST Measurement Results[5]

3. Terminology

3.1 *Definitions*—Refer to Terminology E 170.

4. Summary of Test Method

4.1 This test method describes the determination of the average neutron energy and fluence by use of three activities from a select list of dosimetry reactions. Three dosimetry reactions are chosen based on a number of factors including the intensity of the neutron field, the reaction half-lives, the slope of the dosimetry reaction cross section near 14-MeV, and the minimum time between sensor irradiation and the gamma counting. The activities from these selected reactions are measured. Two of the activities are used, in conjunction with the nuclear data for the dosimetry reactions, to determine the average neutron energy. The third activity is used, along with the neutron energy and nuclear data for the selected reaction, to determine the neutron fluence. The uncertainty of the neutron energy and the neutron fluence is determined from the activity measurement uncertainty and from the nuclear data.

5. Significance and Use

5.1 Refer to Practice E 261 for a general discussion of the measurement of fast-neutron fluence rates with threshold detectors.

5.2 Refer to Test Method E 265 for a general discussion of

[1] This test method is under the jurisdiction of ASTM Committee E10 on Nuclear Technology and Applicationsand is the direct responsibility of Subcommittee E10.07on Radiation Dosimetry for Radiation Effects on Materials and Devices.

Current edition approved June 10, 2002. Published September 2002. Originally published as E 496 – 73. Last previous edition E 496 – 96.

[2] *Annual Book of ASTM Standards*, Vol 12.02.

[3] Available from the International Commission on Radiation Units, 7910 Woodmont Ave., Washington, DC 20014.

[4] Available from American National Standards Institute, 11 W. 42nd St., 13th Floor, New York, NY 10036.

[5] Available from National Institute of Standards and Technology, Gaithersburg, MD 20899.

the measurement of fast-neutron fluence rates by radioactivation of sulfur-32.

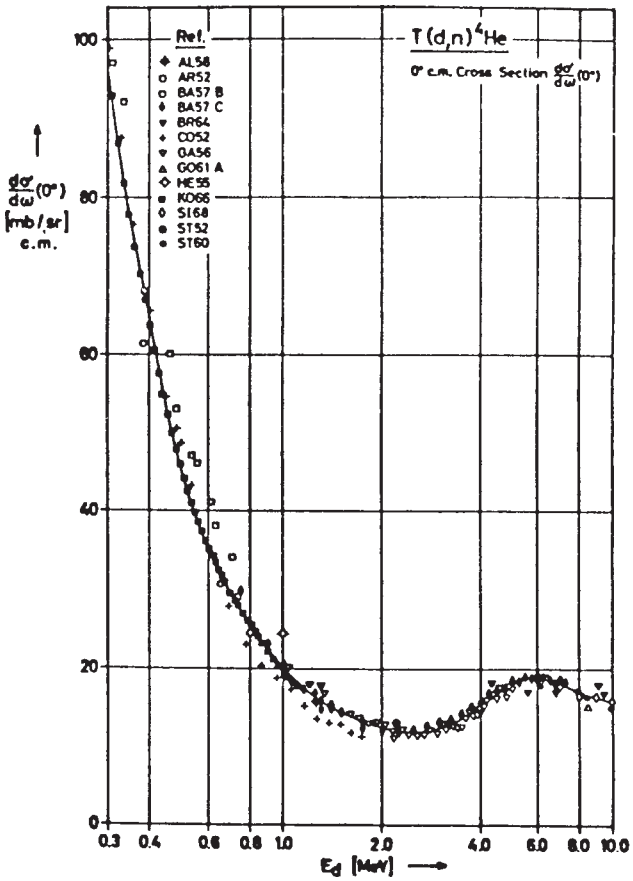

FIG. 1 Variation of 0 Degree $^3H(d,n)^4He$ Differential Cross Section with Incident Deuteron Energy (1)

5.3 Reactions used for the activity measurements can be chosen to provide a convenient means for determining the absolute fluence rates of 14-MeV neutrons obtained with $^3H(d,n)^4He$ neutron generators over a range of irradiation times from seconds to approximately 100 days. High purity threshold sensors referenced in this test method are readily available.

5.4 The neutron-energy spectrum must be known in order to measure fast-neutron fluence using a single threshold detector. Neutrons produced by bombarding a tritiated target with deuterons are commonly referred to as 14-MeV neutrons; however, they can have a range of energies depending on: (*1*) the angle of neutron emission with respect to the deuteron beam, (*2*) the kinetic energy of the deuterons, and (*3*) the target thickness. In most available neutron generators of the Cockroft-Walton type, a thick target is used to obtain high-neutron yields. As deuterons penetrate through the surface and move into the bulk of the thick target, they lose energy, and interactions occurring deeper within the target produce neutrons with correspondingly lower energy.

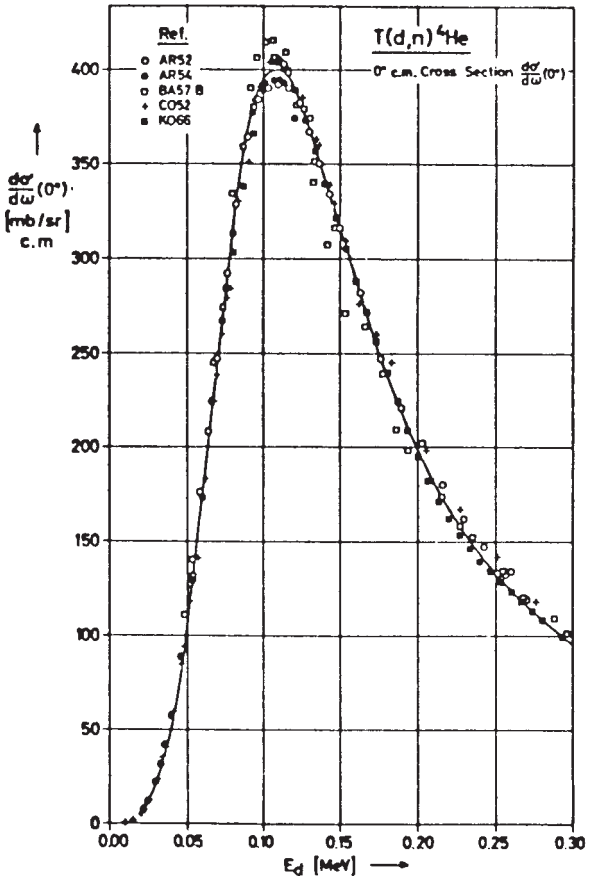

FIG. 2 Variation of 0 Degree $^3H(d,n)^4He$ Differential Cross Section with Incident Deuteron Energy (1)

5.5 Wide variations in neutron energy are not generally encountered in commercially available neutron generators of the Cockroft-Walton type. Figs. 1 and 2 **(1)**[6] show the variation of the zero degree $^3H(d,n)^4He$ neutron production cross section with energy, and clearly indicate that maximum neutron yield is obtained with deuterons having energies near the 107 keV resonance. Since most generators are designed for high yield, the deuteron energy is typically about 200 keV, giving a range of neutron energies from approximately 14 to 15 MeV. The differential center-of-mass cross section is typically parameterized as a summation of Legendre polynomials. Figs. 3 and 4 **(1,2)** show how the neutron yield varies with the emission angle in the laboratory system. The insert in Fig. 4 shows how the magnitude, A_1, of the $P_1(\theta)$ term, and hence the asymmetry in the differential cross section grows with increasing energy of the incident deuteron. The nonrelativistic kinematics (valid for $E_d < 20$ MeV) for the $^3H(d,n)^4He$ reaction show that:

$$E_n^{1/2} = 0.28445E_d^{1/2} \times \cos\theta + \frac{(2.031E_d \times \cos\theta^2 + 352.64228 + 9.95998E_d)^{1/2}}{5.01017} \quad (1)$$

[6] The boldface numbers in parentheses refer to a list of references at the end of this test method.

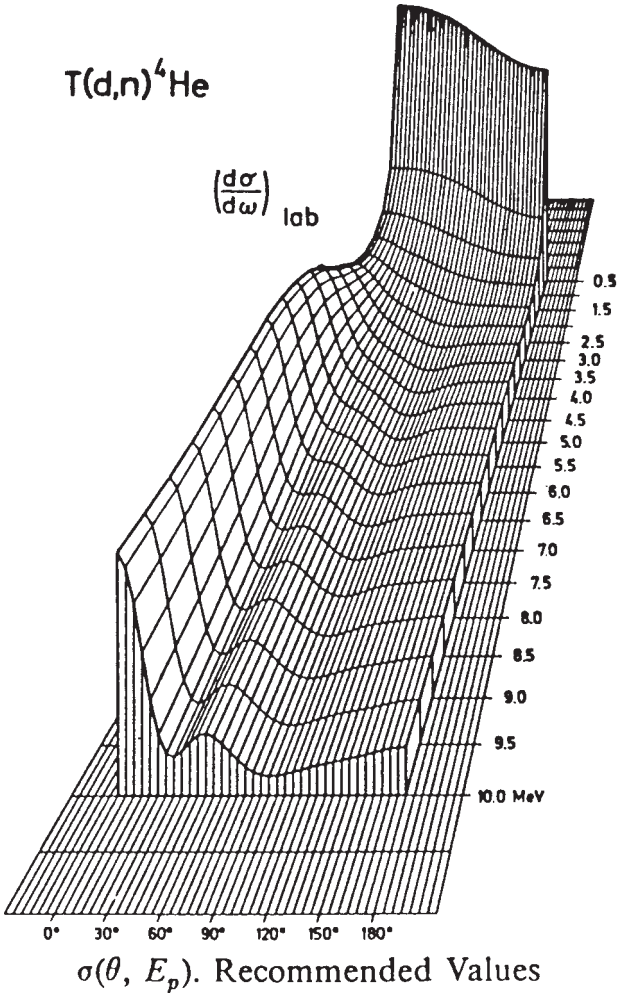

FIG. 3 Energy and Angle Dependence of the ^{3}H(d,n)^{4}He Differential Cross Section (1)

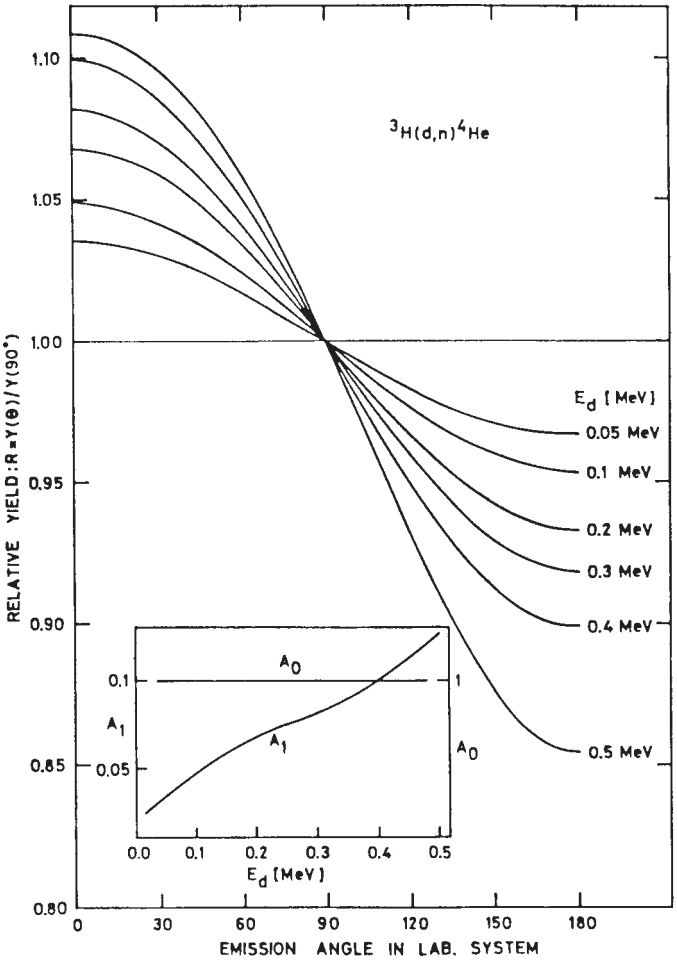

FIG. 4 Change in Neutron Energy From^{3}H(d,n)^{4}He Reaction with Laboratory Emission Angle (2)

where:

E_n = the neutron energy in MeV,
E_d = the incident deuteron energy in MeV, and
θ = the neutron emission angle with respect to the incident deuteron in the laboratory system.

Fig. 5 **(2)** shows how the neutron energy depends upon the angle of scattering in the laboratory coordinate system when the incident deuteron has an energy of 150 keV and is incident on a thick and a thin tritiated target. For thick targets, the incident deuteron loses energy as it penetrates the target and produces neutrons of lower energy. A thick target is defined as a target thick enough to completely stop the incident deuteron. The two curves in Fig. 5, for both thick and thin targets, come from different sources. The dashed line calculations come from Ref **(3)**; the solid curve calculations come from Ref **(4)**; and the measured data come from Ref **(5)**. The dash-dot curve and the right-hand axis gives the difference between the calculated neutron energies for thin and thick targets. Computer codes are available to assist in calculating the expected thick and thin target yield and neutron spectrum for various incident deuteron energies **(21)**.

5.6 The Q-value for the primary ^{3}H(d,n)^{4}He reaction is + 17.59 MeV. When the incident deuteron energy exceeds 3.71 MeV and 4.92 MeV, the break-up reactions ^{3}H(d,np) ^{3}H and ^{3}H(d,2n)^{3}He, respectively, become energetically possible. Thus, at high deuteron energies (>3.71 MeV) this reaction is no longer monoenergetic. Monoenergetic neutron beams with energies from about 14.8 to 20.4 MeV can be produced by this reaction at forward laboratory angles **(6)**.

5.7 It is recommended that the dosimetry sensors be fielded in the exact positions that will be used for the customers of the 14-MeV neutron source. There are a number of factors that can affect the monochromaticity or energy spread of the neutron beam **(6,7)**. These factors include the energy regulation of the incident deuteron energy, energy loss in retaining windows if a gas target is used or energy loss within the target if a solid tritiated target is used, the irradiation geometry, and background neutrons from scattering with the walls and floors within the irradiation chamber.

6. Apparatus

6.1 Either a NaI(Tl) or a Ge semiconductor gamma-ray spectrometer, incorporating a multichannel pulse-height analyzer is required. See Test Methods E 181 for a discussion of spectrometer systems and their use.

6.2 If sulfur is used as a sensor, then a beta particle detector is required. The apparatus required for beta counting of sulfur is described in Test Methods E 181 and E 265.

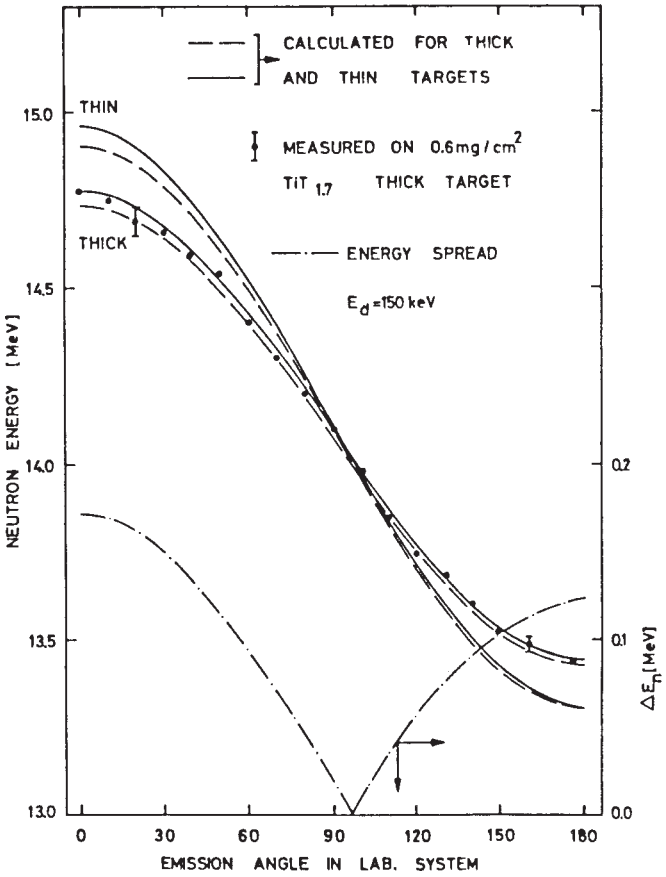

FIG. 5 Dependence of $^{3}H(d,n)^{4}He$ Neutron Energy on Angle (2)

6.3 A precision balance for determining foil masses is required.

7. Materials and Manufacture

7.1 High purity threshold foils are available in a large variety of thicknesses. Foils of suitable diameter can be punched from stock material. Small diameter wire may also be used. Prepunched and weighed high purity foils are also available commercially. Guide E 720 provides some details on typical foil masses and purity. Foils of 12.7 and 25.3 mm (0.50 and 1.00 in.) diameter and 0.13 and 0.25 mm (0.005 and 0.010 in.) thickness are typical.

7.2 See Test Method E 265 for details on the availability and preparation of sulfur sensors.

8. Calibration

8.1 See Test Methods E 181 for general detector calibration methods. Test Methods E 181 addresses both gamma-ray spectrometers and beta counting methods.

9. Procedure for Determining the Neutron Energy

9.1 *Selection of Sensors*:

9.1.1 Use of an activity ratio method is recommended for the determination of the neutron energy. The activity ratio method has been described in Ref **(8)**. This test method has been validated for ENDF/B-VI cross sections **(9)** in Ref **(10)**.

9.1.2 Sensor selection depends upon the length of the irradiation, the cross section for the relevant sensor reaction, the reaction half-life, and the expected fluence rate. Table 1 lists some dosimetry-quality reactions that are useful in the 14-MeV energy region. The short half-lives of some of these reaction products, such as ^{27}Mg and ^{62}Cu, generally limit the use of these activation products to irradiation times of less than about 15 min. Table 2 and Fig. 6 show the recommended cross sections, in the vicinity of 14-MeV, for these reactions. The cross sections recommended in Table 1 are from the ENDF/B-VI and IRDF-90 **(15)** cross section compilations. The SNLRML cross section compendium **(16)** is a single-point-of-reference source for the recommended cross sections and uncertainty data for the reactions mentioned in Table 1. The references for the nuclear data in Table 1 are given in the table.

9.1.3 Longer high fluence irradiations are recommended for the determination of the neutron energy. Table 3 and Figs. 7 and 8 show the neutron energy-dependent activity ratios for some commonly used sensor combinations. In general, the steeper the activity ratio, the more sensitive the method is to the neutron energy.

9.1.4 Table 4 shows the energy resolutions of some specific sensor combinations for a 14.5 MeV neutron source. The $^{54}Fe(n,p)^{54}Mn/^{58}Ni(n,2n)^{57}Ni$ and $^{27}Al(n,\alpha)^{24}Na/^{58}Ni(n,2n)^{57}Ni$ are recommended sensor combinations due to their steep slope and their very accurate dosimetry cross section evaluations.

9.2 *Determine the Sensor Mass*—Weigh each sensor to a precision of 0.1 %. Nonuniform foil thicknesses can result from the use of dull punches and frequently result in weight variation of 10 % or more.

9.3 *Irradiation of Sensors*—Irradiate the sensors, making certain that both sensors experience exactly the same fluence. The fluence gradients near a 14-MeV source tend to be high and it may be necessary to stack the sensors together or to mount them on a rotating disk during irradiation. Note the length of the irradiation, t_i, and the time the irradiation ended. Some sensors may have an interference reaction that is sensitive to low energy neutrons. The interference reaction may be associated with the primary sensor element or with a contaminant material in the sensor. Of the reactions listed in Table 1, the use of a Cu sensor is the only case where the primary sensor element may be responsible for an interference reaction. In this case the useful $^{65}Cu(n,2n)^{64}Cu$ reaction activity must be distinguished from the $^{63}Cu(n,\gamma)^{64}Cu$ interference reaction activity (for example, by using an isotopically pure sensor or by experimentally verifying bounds on the maximum possible level of interference). Other examples of interference reactions from contaminant materials include trace impurities of Mn in Fe sensors and Na in Al sensors. Manganese is a frequent contaminant in Fe foils. In this case the $^{55}Mn(n,\gamma)^{56}Mn$ reaction interferes with the desired sensor response from the $^{56}Fe(n,p)^{56}Mn$ reaction. Salt from handling Al sensors can result in the $^{23}Na(n,\gamma)^{24}Na$ contaminant reaction which affects the use of the $^{27}Al(n,\alpha)^{24}Na$ dosimetry sensor. If one is uncertain about the importance of an interference reaction that has a high thermal neutron cross section, it is recommended that the sensor be irradiated with and without a cadmium cover to quantify the importance of this interference term.

TABLE 1 Cross Section Parameters for Some Useful Reactions

	Dosimetry Reactions	Target Nucleus					Product Nucleus			Reaction Notes
		Elemental Atomic Weight **(12, 12)**	Isotopic Atomic Number Abundance, % **(12,)**	Cross Section Source		Cross Section Uncertainty Near 14-MeV, %	Half-Life **(12,**	E_γ, keV **(11)**	Yield, %, γ per Reaction **(11)**	
				Library	Material Number					
1	$^{24}Mg(n,p)^{24}Na$	24.3050	78.99	IRDF-90	1225	0.5	14.9512 h	1368.633	100.0	...
								2754.028	99.944	...
2	$^{27}Al(n,p)^{27}Mg$	26.981539	100.0	IRDF-90	1325	15.6	9.458 m	843.76	71.8	A
								1014.46	28.0	...
3	$^{27}Al(n,\alpha)^{24}Na$	26.981539	100.0	IRDF-90	1325	0.4	14.9512 h	1368.633	100.0	...
								2754.028	99.944	...
4	$^{32}S(n,p)^{32}P$	32.065	95.02	IRDF-90	1625	8.0	14.262 d	$<E_\beta> = 695$	100.0	B
5	$^{54}Fe(n,p)^{54}Mn$	55.845	5.845	ENDF/B-VI	2625	3.0	312.11 d	834.848	99.976	...
6	$^{56}Fe(n,p)^{56}Mn$	55.845	91.754	ENDF/B-VI	2631	2.1	2.5789 h	846.754	98.87	...
								1810.72	27.189	...
								2113.05	14.336	...
7	$^{58}Ni(n,p)^{58}Co$	58.6934	68.077	ENDF/B-VI	2825	18.6	70.86 d	810.7593	99.45	...
							9.04 h (meta)	863.951	0.69	...
								1674.725	0.52	...
								24.889	0.0369	...
8	$^{58}Ni(n,2n)^{57}Ni$	58.6934	68.077	ENDF-B-VI	2825	2.4	35.60 h	1377.63	81.7	...
								1919.52	12.255	...
9	$^{63}Cu(n,2n)^{62}Cu$	63.546	69.17	IRDF-90	2925	1.5	9.67 m	1173.02	0.335	A,C
								875.71	0.1499	...
10	$^{63}Cu(n,\alpha)^{60}Co$	63.546	69.17	ENDF/B-VI	2925	6.0	1925.15 d	1173.228	99.85	...
								1332.492	99.9826	...
							10.467 m	58.603	2.01	...
							(meta)	826.28	0.00768	...
								1332.501	0.24	...
								2158.77	0.00072	...
11	$^{65}Cu(n,2n)^{64}Cu$	63.546	30.83	ENDF/B-VI	2931	2.8	12.700 h	1345.79	0.48	...
12	$^{64}Zn(n,p)^{64}Cu$	65.39	48.6	IRDF-90	3025	3.4	12.700 h	1345.79	0.48	...
13	$^{90}Zr(n,2n)^{89}Zr$	91.224	51.45	IRDF-90	4025	1.0	784.41 h	909.15	99.04	...
								1713.0	0.7447808	...
								1744.5	0.1228096	...
							4.161m (meta)	587.70	89.5	...
								1507.4	6.075	
14	$^{93}Nb(n,2n)^{92m}Nb$	92.90638	100.0	IRDF-90	4125	1.5	10.15 d	934.44	99.07	D
								912.6	1.78326	...
								1847.5	0.852	...

A Use of this reaction requires accurate timing but also provides high specific activity per neutron.
B The β emissions are counted to determine the activity.
C Use of 511 keV line risks high background signals from other positron emitters.
D The cross section is particularly flat near 14-MeV, insensitive to neutron energy, and hence suitable for the measurement of fluence.

9.4 *Determination of Sensor Activity*—Guide E 720 provides details on the calculational procedure for determining the activity of an irradiated sensor. The results of this step should be the activities, corrected to a time corresponding to the end of the irradiation. The activity should be corrected for decay during the irradiation, as explained in Guide E 720. This decay correction is especially important for short half-life reactions. The activity should have units of Bq per target atom.

9.5 *Calculations*—Section 11 details the calculations that use these two sensor activities to determine the neutron average energy.

10. Procedure for Determining the Neutron Fluence

10.1 *Selection of Sensor*:

10.1.1 To avoid sensitivity to uncertainty in the exact neutron energy, the 14-MeV neutron fluence sensor is generally chosen to have a flat response in the 13 MeV to 15 MeV energy region. Fig. 6 and Table 2 show the energy dependence near 14 MeV for some frequently used dosimetry sensors. An examination of Fig. 6 and Table 2 clearly indicates a strong preference to use the $^{93}Nb(n,2n)^{92m}Nb$ reaction. This preference is based on the flat energy response and the small cross section uncertainty near 14 MeV. The $^{93}Nb(n,2n)^{92m}Nb$ reaction has been used as a transfer standard for 14-MeV sources by national standards laboratories **(17)** and in international intercomparisons **(18)**. The footnotes in Table 1 list some precautions about use of some other reactions. If the $^{93}Nb(n,2n)^{92m}Nb$ reaction cannot be used in a specific case, the uncertainty of the $^{3}H(d,n)^{4}He$ neutron energy, as determined from Section 9, should be used in conjunction with Table 2 and Fig. 6 to determine the best alternative reaction.

10.1.2 Paragraph 9.1.2 indicates some other considerations in the choice of a dosimetry fluence reaction based on the irradiation length and expected strength.

10.2 *Determine the Sensor Mass*—Weigh the sensor to a precision of 0.1 %. Nonuniform foil thicknesses can result from the use of dull punches and frequently result in weight variations of 10 % or more.

10.3 *Irradiation of Sensor*—Paragraph 9.3 provides details and precautions on the irradiation of the sensor.

10.4 *Determination of Sensor Activity*—Guide E 720 provides details on the calculational procedure for determining the activity on an irradiated sensor. The result of this step should be

TABLE 2 Cross Section Near 14-MeV for Dosimetry Reactions

Energy (MeV)		Ratio						
		$^{24}Mg(n,p)^{24}Na$	$^{27}Al(n,p)^{27}Mg$	$^{27}Al(n,\alpha)^{24}Na$	$^{32}S(n,p)^{32}P$	$^{54}Fe(n,p)^{54}Mn$	$^{56}Fe(n,p)^{56}Mn$	$^{58}Ni(n,p)^{58}Co$
1	13.55	0.20894E + 00	0.76781E−01	0.12545E + 00	0.28764E + 00	0.37868E + 00	0.11683E + 00	0.42123E + 00
2	13.65	0.20581E + 00	0.75983E−01	0.12488E + 00	0.28009E + 00	0.37045E + 00	0.11676E + 00	0.41075E + 00
3	13.75	0.20055E + 00	0.75185E−01	0.12384E + 00	0.27253E + 00	0.36222E + 00	0.11670E + 00	0.40027E + 00
4	13.85	0.19314E + 00	0.74387E−01	0.12278E + 00	0.26498E + 00	0.35400E + 00	0.11628E + 00	0.38979E + 00
5	13.95	0.19116E + 00	0.73589E−01	0.12258E + 00	0.25743E + 00	0.34577E + 00	0.11551E + 00	0.37931E + 00
6	14.05	0.19460E + 00	0.72791E−01	0.12220E + 00	0.25069E + 00	0.33806E + 00	0.11474E + 00	0.36882E + 00
7	14.15	0.19642E + 00	0.71993E−01	0.12151E + 00	0.24476E + 00	0.33088E + 00	0.11398E + 00	0.35834E + 00
8	14.25	0.19661E + 00	0.71195E−01	0.12043E + 00	0.23883E + 00	0.32369E + 00	0.11306E + 00	0.34785E + 00
9	14.35	0.19508E + 00	0.70397E−01	0.11808E + 00	0.23290E + 00	0.31650E + 00	0.11200E + 00	0.33736E + 00
10	14.45	0.19184E + 00	0.69599E−01	0.11614E + 00	0.22697E + 00	0.30933E + 00	0.11094E + 00	0.32689E + 00
11	14.55	0.18751E + 00	0.68800E−01	0.11482E + 00	0.22268E + 00	0.30214E + 00	0.10988E + 00	0.31725E + 00
12	14.65	0.18211E + 00	0.68002E−01	0.11330E + 00	0.22001E + 00	0.29496E + 00	0.10871E + 00	0.30848E + 00
13	14.75	0.17714E + 00	0.67204E−01	0.11220E + 00	0.21735E + 00	0.28777E + 00	0.10743E + 00	0.29971E + 00
14	14.85	0.17259E + 00	0.66406E−01	0.11102E + 00	0.21469E + 00	0.28059E + 00	0.10615E + 00	0.29092E + 00
15	14.95	0.17054E + 00	0.65608E−01	0.10969E + 00	0.21202E + 00	0.27339E + 00	0.10487E + 00	0.28217E + 00
16	15.05	0.17097E + 00	0.64755E−01	0.10878E + 00	0.20836E + 00	0.26708E + 00	0.10333E + 00	0.27340E + 00
17	15.15	0.17140E + 00	0.63846E−01	0.10787E + 00	0.20370E + 00	0.26165E + 00	0.10151E + 00	0.26463E + 00
18	15.25	0.17138E + 00	0.62938E−01	0.10674E + 00	0.19905E + 00	0.25622E + 00	0.99689E−01	0.25586E + 00
19	15.35	0.16864E + 00	0.62029E−01	0.10508E + 00	0.19439E + 00	0.25080E + 00	0.97875E−01	0.24709E + 00
20	15.45	0.16546E + 00	0.61120E−01	0.10340E + 00	0.18973E + 00	0.24537E + 00	0.96058E−01	0.23832E + 00
21	15.55	0.16227E + 00	0.60212E−01	0.10171E + 00	0.18508E + 00	0.23994E + 00	0.94262E−01	0.22955E + 00
Energy (MeV)		Reaction						
		$^{58}Ni(n,2n)^{57}Ni$	$^{63}Cu(n,2n)^{62}Cu$	$^{63}Cu(n,\alpha)^{60}Co$	$^{65}Cu(n,2n)^{64}Cu$	$^{64}Zn(n,p)^{64}Cu$	$^{90}Zr(n,2n)^{89}Zr$	$^{93}Nb(n,2n)^{92m}Nb$
1	13.55	0.13385E−01	0.37647E + 00	0.44060E−01	0.83059E + 00	0.20144E + 00	0.44720E + 00	0.45691E + 00
2	13.65	0.15248E−01	0.39166E + 00	0.43980E−01	0.84498E + 00	0.19609E + 00	0.48245E + 00	0.45756E + 00
3	13.75	0.17482E−01	0.40670E + 00	0.43869E−01	0.85935E + 00	0.19074E + 00	0.51698E + 00	0.45807E + 00
4	13.85	0.19669E−01	0.42083E + 00	0.43575E−01	0.87373E + 00	0.18539E + 00	0.55079E + 00	0.45842E + 00
5	13.95	0.21811E−01	0.43480E + 00	0.43250E−01	0.88812E + 00	0.18004E + 00	0.58251E + 00	0.45877E + 00
6	14.05	0.23808E−01	0.44878E + 00	0.42752E−01	0.90066E + 00	0.17469E + 00	0.61213E + 00	0.45913E + 00
7	14.15	0.25660E−01	0.46275E + 00	0.42082E−01	0.91136E + 00	0.16934E + 00	0.64245E + 00	0.45948E + 00
8	14.25	0.27809E−01	0.47681E + 00	0.41433E−01	0.92206E + 00	0.16460E + 00	0.67346E + 00	0.45978E + 00
9	14.35	0.30257E−01	0.49138E + 00	0.40919E−01	0.93276E + 00	0.16348E + 00	0.70327E + 00	0.45980E + 00
10	14.45	0.32818E−01	0.50604E + 00	0.40429E−01	0.94344E + 00	0.16297E + 00	0.73186E + 00	0.45977E + 00
11	14.55	0.35502E−01	0.52069E + 00	0.39909E−01	0.95218E + 00	0.16246E + 00	0.75760E + 00	0.45973E + 00
12	14.65	0.37466E−01	0.53535E + 00	0.39359E−01	0.95891E + 00	0.16157E + 00	0.78048E + 00	0.45970E + 00
13	14.75	0.38696E−01	0.54968E + 00	0.38807E−01	0.96566E + 00	0.15972E + 00	0.80093E + 00	0.45958E + 00
14	14.85	0.39979E−01	0.56207E + 00	0.38243E−01	0.97238E + 00	0.15788E + 00	0.81894E + 00	0.45889E + 00
15	14.95	0.41567E−01	0.57415E + 00	0.37675E−01	0.97912E + 00	0.15716E + 00	0.83770E + 00	0.45811E + 00
16	15.05	0.43211E−01	0.58622E + 00	0.37072E−01	0.98554E + 00	0.15688E + 00	0.85720E + 00	0.45733E + 00
17	15.15	0.44855E−00	0.59830E + 00	0.36432E−01	0.99165E + 00	0.15661E + 00	0.87671E + 00	0.45656E + 00
18	15.25	0.46499E−01	0.61088E + 00	0.35786E−01	0.99777E + 00	0.15633E + 00	0.89596E + 00	0.45578E + 00
19	15.35	0.48144E−01	0.62654E + 00	0.35121E−01	0.10039E + 01	0.15606E + 00	0.91372E + 00	0.45500E + 00
20	15.45	0.49788E−01	0.64272E + 00	0.34450E−01	0.10100E + 01	0.15579E + 00	0.93123E + 00	0.45422E + 00
21	15.55	0.51303E−01	0.65889E + 00	0.33771E−01	0.10148E + 01	0.15385E + 00	0.94874E + 00	0.45293E + 00

the activity, corrected to a time corresponding to the end of the irradiation, for the sensor selected in 10.1. The activity should be corrected for decay during the irradiation, as explained in Guide E 720. The activity should have units of Bq per target atom.

10.5 *Calculations*—Section 12 details the calculations that use the sensor activity, in conjunction with the average neutron energy, to determine the neutron fluence.

11. Calculation of Neutron Energy

11.1 Form the ratio of the measured activities determined in 9.4 for the two sensor reactions chosen in 9.1. Refer to this ratio as R_{act}:

$$R_{act} = \frac{A_1}{A_2} \tag{2}$$

where:

A_1 = the activity from the first reaction, and
A_2 = the activity from the second reaction.

In this test method the numerical subscripts 1 and 2 will occur on various quantities. Unless there is an explicit definition, these subscripts refer to the two reactions chosen in 9.1.

11.2 Use the reaction half-lives from Table 1 to convert the activity ratio into a cross section ratio, R_{xsec}.

$$R_{xsec} = R_{act} \times \frac{\tau_1}{\tau_2} = \frac{A_1}{A_2} \times \frac{\tau_1}{\tau_2} \tag{3}$$

11.3 Determine the energy that corresponds to the cross section ratio, R_{xsec}.

11.3.1 Use the data in Table 3 and linear-linear interpolation to determine the neutron energy that corresponds to this cross

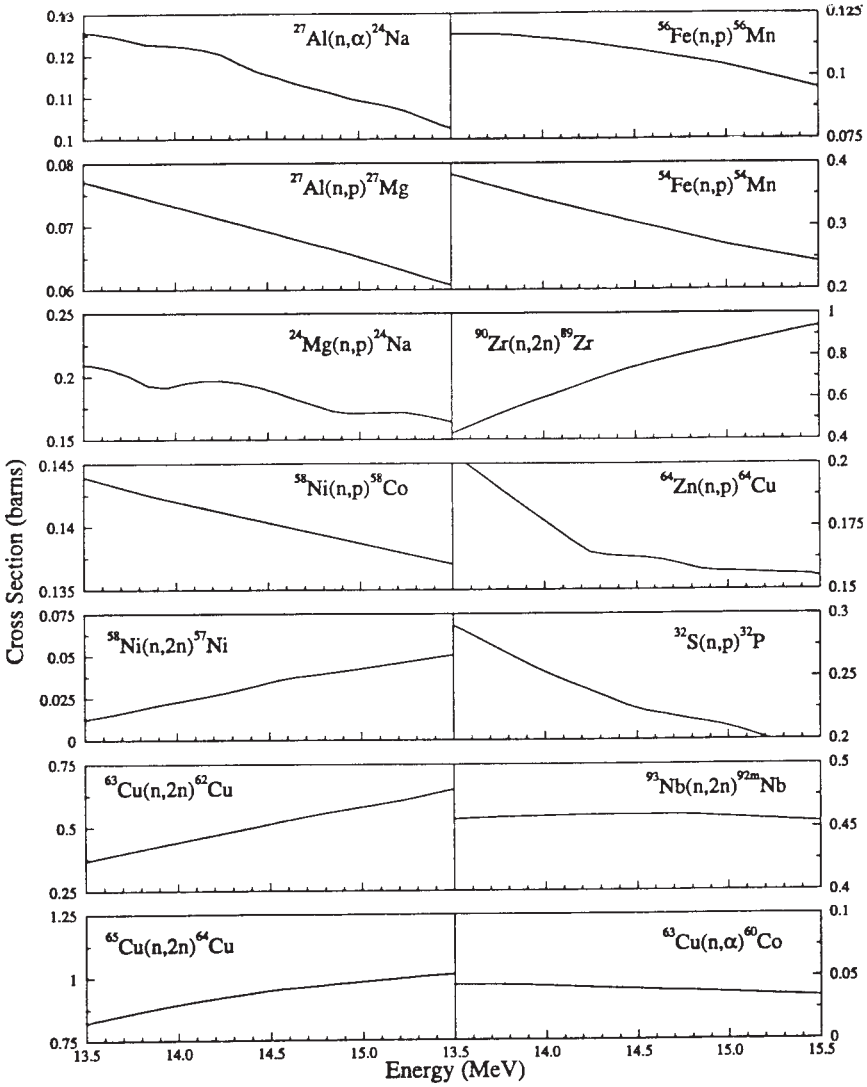

FIG. 6 Cross Sections for Several Reactions Useful for 14-MeV Dosimetry

section ratio. Refer to this energy as E_{eff}. This energy represents an average energy for the neutrons. The neutron energy from a thick target is not truly monoenergetic.

11.3.2 If the dosimetry-quality sensor chosen is not addressed in Table 3, then the experimenter must construct data similar to that presented in Table 3 from a dosimetry-quality cross section evaluation for the reactions used. A necessary component of dosimetry-quality cross sections is the presence of covariance data. The methodology used in this test method makes use of the cross section uncertainty. This test method requires the existence of a complete covariance matrix even though the off-diagonal covariance elements are not utilized. This requirement is made to ensure that a dosimetry-quality cross section evaluation is used. Single point cross section values with uncertainties are not sufficient since the energy-dependent slope of the cross section must be known. All high-quality cross section determinations that address more than a single energy have been observed to provide a state-of-the-art statistical analysis that includes a covariance matrix. The International Reactor Dosimetry File (IRDF-90) **(15)** or a cross section in the SNLRML compendium **(16)** are recommended as sources for cross section data.

11.4 Determine the slope of the cross section ratio near the expected neutron energy, E_{eff}.

11.4.1 Use Table 3 to determine the slope of the cross section ratio (change in cross section ratio divided by the change in neutron energy) for the energy E_{eff}. The slope is referred to as S_{eff}.

11.4.2 The slope is not intended to represent a derivative of a curve fit to the cross section data evaluated at a particular energy point. The slope should be indicative of the general behavior of the cross section in the energy region of interest. Fig. 6 shows plots of the data from Table 3. If the slope is not smooth in the energy region of interest, the user should select a different dosimetry reaction. For example, the $^{64}Zn(n,p)^{64}Cu$ cross section shows a discontinuity in the cross section slope near 14.25 MeV. This reaction should not be used for a neutron energy determination in this energy region. The $^{64}Zn(n,p)^{64}Cu$ reaction may still be useful for the neutron fluence determination.

11.4.3 If the sensors chosen are not represented in Table 3,

TABLE 3 Dosimetry Cross Section Ratios Near 14-MeV

Energy (MeV)		Reaction Ratio					
		$^{58}Ni(n,p)/^{58}Ni(n,2n)$	$^{54}Fe(n,p)/^{58}Ni(n,2n)$	$^{27}Al(n,\alpha)/^{58}Ni(n,2n)$	$^{27}Al(n,p)/^{63}Cu(n,2n)$	$^{63}Cu(n,\alpha)/^{65}Cu(n,2n)$	$^{27}Al(n,p)/^{65}Cu(n,2n)$
1	13.55	0.31470E + 02	0.28291E + 02	0.93724E + 01	0.20395E + 00	0.53047E−01	0.92442E−01
2	13.65	0.26938E + 02	0.24295E + 02	0.81899E + 01	0.19400E + 00	0.52049E−01	0.89923E−01
3	13.75	0.22896E + 02	0.20720E + 02	0.70839E + 01	0.18487E + 00	0.51049E−01	0.87491E−01
4	13.85	0.19817E + 02	0.17998E + 02	0.62423E + 01	0.17676E + 00	0.49872E−01	0.85137E−01
5	13.95	0.17391E + 02	0.15853E + 02	0.56201E + 01	0.16925E + 00	0.48698E−01	0.82859E−01
6	14.05	0.15491E + 02	0.14199E + 02	0.51327E + 01	0.16220E + 00	0.47467E−01	0.80820E−01
7	14.15	0.13965E + 02	0.12895E + 02	0.47354E + 01	0.15558E + 00	0.46175E−01	0.78995E−01
8	14.25	0.12509E + 02	0.11640E + 02	0.43306E + 01	0.14932E + 00	0.44935E−01	0.77213E−01
9	14.35	0.11150E + 02	0.10460E + 02	0.39026E + 01	0.14326E + 00	0.43869E−01	0.75472E−01
10	14.45	0.99607E + 01	0.94256E + 01	0.35389E + 01	0.13754E + 00	0.42853E−01	0.73772E−01
11	14.55	0.89361E + 01	0.85105E + 01	0.32342E + 01	0.13213E + 00	0.41913E−01	0.72255E−01
12	14.65	0.82336E + 01	0.78727E + 01	0.30241E + 01	0.12702E + 00	0.41046E−01	0.70916E−01
13	14.75	0.77452E + 01	0.74367E + 01	0.28995E + 01	0.12226E + 00	0.40187E−01	0.69594E−01
14	14.85	0.72768E + 01	0.70184E + 01	0.27770E + 01	0.11815E + 00	0.39329E−01	0.68292E−01
15	14.95	0.67883E + 01	0.65771E + 01	0.26389E + 01	0.11427E + 00	0.38478E−01	0.67007E−01
16	15.05	0.63271E + 01	0.61808E + 01	0.25174E + 01	0.11046E + 00	0.37616E−01	0.65705E−01
17	15.15	0.58997E + 01	0.58332E + 01	0.24049E + 01	0.10671E + 00	0.36739E−01	0.64384E−01
18	15.25	0.55025E + 01	0.55102E + 01	0.22955E + 01	0.10303E + 00	0.35866E−01	0.63079E−01
19	15.35	0.51323E + 01	0.52094E + 01	0.21826E + 01	0.99002E−01	0.34985E−01	0.61788E−01
20	15.45	0.47867E + 01	0.49283E + 01	0.20768E + 01	0.95096E−01	0.34109E−01	0.60515E−01
21	15.55	0.44744E + 01	0.46769E + 01	0.19825E + 01	0.91384E−01	0.33278E−01	0.59334E−01

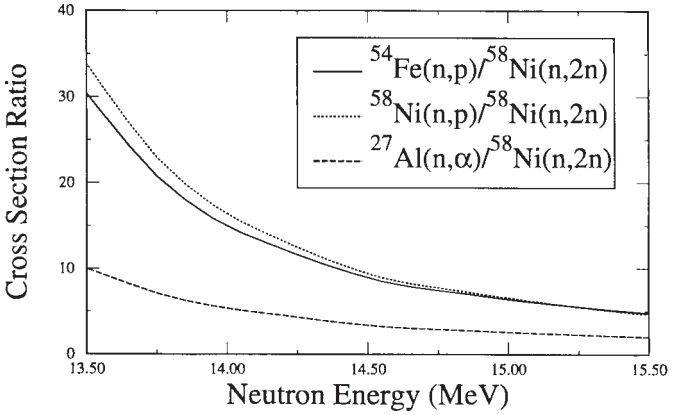

FIG. 7 Ratios of Cross Section for $^3H(d,n)^4He$ Neutron Energy Determination

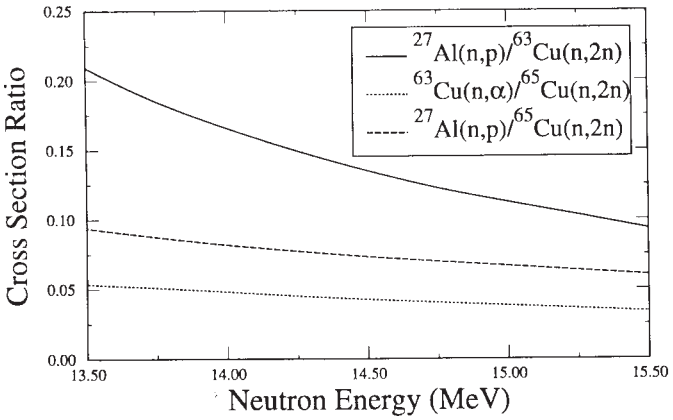

FIG. 8 Ratios of Cross Section for $^3H(d,n)^4He$ Neutron Energy Determination

then follow the guidance in 11.3.2 to obtain the recommended nuclear data.

11.5 The uncertainty in the activity ratio directly affects the uncertainty in the neutron energy determination. Use the uncertainties in the two activity measurements and the uncertainty in the evaluated cross sections to calculate the uncertainty in the neutron energy.

11.5.1 Determine the measurement uncertainty component of the activity ratio, δR_{act}. The normal theory for the propagation of errors can be applied to Eq 2 in order to determine δR_{act}. If the two activity measurements are uncorrelated, then the ratio uncertainty is the root-mean-squared (RMS) value of the two activity uncertainties.

11.5.2 From Eq 3 and the fact that the uncertainty of reaction half-lives is very small, it is clear that the percent uncertainty in the activity ratio, δR_{act}, is the same as the percent uncertainty in the cross section ratio. The uncertainty in the cross section ratio will be denoted by δR_{xsec}.

11.5.3 Use the projection technique indicated in Fig. 9 to determine the neutron energy uncertainty that corresponds to the measurement uncertainty in the cross section ratio. This is one component of the neutron energy uncertainty. This component will be referred to as $\Delta^{eng}{}_1$ and is given by:

$$\Delta^{eng}{}_1 = \left| \frac{\delta R_{xsec}}{S_{eff}} \right| \tag{4}$$

where:

S_{eff} = the slope of the cross section ratio determined in 11.4.

11.5.4 Dosimetry-quality covariance data shall be available for any cross section evaluation used. Cross-reaction covariance data is not typically available for the selected reactions. However, if this data is available, it should be used. This cross section uncertainty data should be used to estimate the uncertainty in the evaluated cross section near E_{eff}. This uncertainty is referred to as δR_{eff}. The same projection technique detailed in 11.5.3 shall be used to convert this uncertainty into a cross section uncertainty component for the neutron energy, $\Delta^{eng}{}_2$. This component is given by:

$$\Delta^{eng}{}_2 = \left| \frac{\delta R_{eff}}{S_{eff}} \right| \tag{5}$$

Table 1 gives cross section uncertainty data for many useful dosimetry sensors in the 14-MeV energy region. Table 4 gives

TABLE 4 Energy Resolution from Ratios of the Cross Sections

NOTE 1— * = Number of digits given is to provide traceability to the calculations and does not imply a numerical accuracy.
= Slope calculated as the change in the ratio over the energy interval from 14.25 MeV to 14.75 MeV divided by the energy interval (0.5 MeV).
@ = Uncertainty is computed as the rms average of the individual cross section uncertainties at 14.5 MeV as provided in the covariance in the appropriate cross section evaluation.

	Cross Section Ratio	Ratio* at 14.5 MeV (R_{xsec})	Uncertainty@ in Ratio* (δR_{xsec})	Slope#* Near 14.5 MeV (MeV^{-1}) (S_{eff})	Energy Resolution*		Comment
					Cross Section Bias Uncertainty (MeV) ($\Delta^{eng}{}_2$)	Uncertainty for 4 % Counting Statistics (MeV) ($\Delta^{eng}{}_1$)	
1	$^{58}Ni(n,p)/^{58}Ni(n,2n)$	9.428	18.7 %	9.5276	0.19	0.06	A
2	$^{54}Fe(n,p)/^{58}Ni(n,2n)$	8.950	3.7 %	8.4066	0.04	0.06	B
3	$^{27}Al(n,\alpha)/^{58}Ni(n,2n)$	3.381	2.3 %	8.0813	0.01	0.02	B
4	$^{27}Al(n,p)/^{63}Cu(n,2n)$	0.1348	15.7 %	0.05412	0.39	0.14	C,A,D
5	$^{63}Cu(n,\alpha)/^{65}Cu(n,2n)$	0.04238	6.6 %	0.009496	0.29	0.25	D
6	$^{27}Al(n,p)/^{65}Cu(n,2n)$	0.07301	15.9 %	0.015238	0.76	0.27	C,A,D

A Large uncertainty in cross section ratio results in large energy resolution uncertainty.
B Recommended reaction ratio.
C Very fast decay time for cross sections makes accurate counting difficult.
D Very flat slope increases the energy uncertainty.

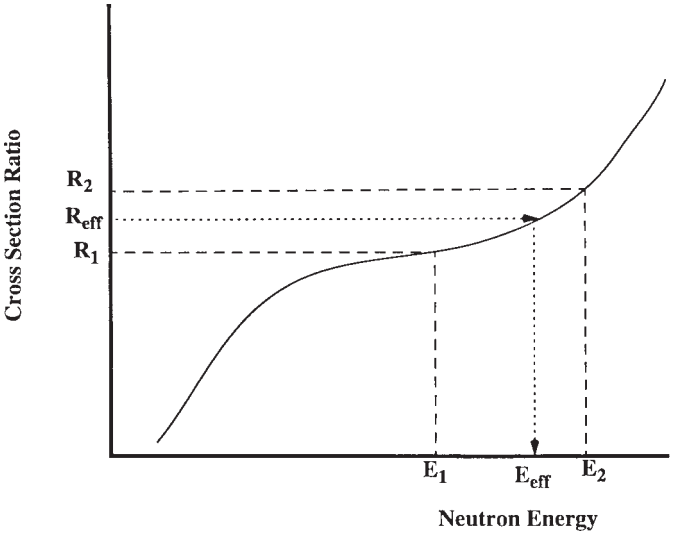

FIG. 9 Interpolation of Neutron Energy

some examples of the uncertainty in the cross section ratio at 14.5 MeV for selected reaction ratios.

11.5.5 The total uncertainty in the activity ratio is obtained by adding in quadrature the cross section uncertainty, $\Delta^{eng}{}_2$, with the measurement uncertainty, $\Delta^{eng}{}_1$ to obtain the uncertainty in the neutron energy determination.

$$\Delta^{eng} = \sqrt{\Delta^{eng}{}_1{}^2 + \Delta^{eng}{}_2{}^2} \tag{6}$$

Table 4 gives some representative values for the two components of the neutron energy uncertainty for several cross section ratios.

11.6 *Example Calculation*—To illustrate the method, assume that the experimental procedure in Section 9 resulted in the selection of $^{54}Fe(n,p)^{54}Mn$ and $^{58}Ni(n,2n)^{57}Ni$ sensors with measured activities of $7.88 \times 10^{-23} \pm 6.5$ % Bq/atom and $1.85 \times 10^{-21} \pm 3.0$ % Bq/atom, respectively.

11.6.1 The activity ratio is given by $R_{act} = 7.88 \times 10^{-23}/1.85 \times 10^{-21} = 4.26 \times 10^{-2}$.

11.6.2 The cross section ratio is given by:

$$R_{xsec} = \frac{7.88 \times 10^{-23}}{1.85 \times 10^{-21}} \times \frac{312.12 \times 24}{35.65} = 8.95 \tag{7}$$

11.6.3 From the data in Table 3, E_{eff} is between 14.45 and 14.55. Linear interpolation gives:

$$E_{eff} = E_{10} + (R_{xsec} - R_{10}) \times (E_{11} - E_{10})/(R_{11} - R_{10})$$

$$= 14.45 + (8.95 - 9.4256) \times (14.55 - 14.45)/(8.5105 - 9.4256)$$
$$= 14.45 + 0.05197$$
$$\cong 14.50\ MeV \tag{8}$$

where:
E_i = the energy from Table 3,
R_i = the $^{54}Fe(n,p)/^{58}Ni(n,2n)$ cross section ratio from Table 3, and
the subscripts 10 and 11 = the Table 3 entry numbers.

11.6.4 Table 3 shows that the slope of the cross section ratio near E_{eff} is $S_{eff} = (7.4367 - 11.64)/(14.75 - 14.25) = -8.4066$ MeV^{-1}. Fig. 6 shows that both the cross sections have a fairly smooth slope near 14.5 MeV. Since the neutron energy spread can be greater than 0.2 MeV (the difference between the thick and thin target average neutron energy from Fig. 5), the slope should be evaluated over an interval larger than 0.2 MeV. Considering the smooth slope in Fig. 6 and the tabulated values available from Table 3, the energy values of 14.25 and 14.75 MeV were chosen in this example to evaluate the slope.

11.6.5 The measurement uncertainty of the activity ratio is given by the RMS value for the two activity uncertainties. $\delta R_{act} = sqrt([6.5\ \%]^2 + [3.0\ \%]^2) = 7.16$ %.

11.6.6 The percent uncertainty in the cross section ratio is the same as the percent uncertainty in the activity ratio. $\delta R_{xsec} = \delta R_{act} = 7.16\ \% = 0.0716 \times 8.95 = 0.64082$.

11.6.7 The neutron energy uncertainty component due to the measurement uncertainty is given by $\Delta^{eng}{}_1 = |0.64082/(-8.4066)| = 0.076$ MeV.

11.6.8 Using the data in Table 4 the cross section uncertainty component for the cross section ratio is $\delta R_{xsec} = 3.7\ \% = (0.037) \times (8.95) = 0.33115$.

11.6.9 The neutron energy uncertainty component due to the cross section uncertainty is given by $\Delta^{eng}{}_2 = |0.33115/$

(−8.4066)| = 0.0394 MeV.

11.6.10 The total uncertainty in the neutron energy is given by the RMS value of $\Delta^{eng}{}_1$ and $\Delta^{eng}{}_2$. Δ^{eng} = sqrt(0.076^2 + 0.0394^2) = 0.0856 MeV.

12. Calculation of Neutron Fluence

12.1 Using the activity for the monitor reaction, determine the neutron fluence.

12.1.1 For the monitor reaction selected in 10.1, take the activity determined in 10.4. Refer to this activity as A_{flu}. The activity should have units of Bq per target atom in the monitor sensor.

12.1.2 For the neutron energy determined in Section 11, referred to as E_{eff}, use Table 2 or Fig. 6 to determine the cross section for the reaction chosen. Refer to this cross section as σ_{flu}. The cross section should have units of barns per incident neutron.

12.1.3 The neutron fluence is given by:

$$\Phi = \frac{A_{flu} \times 10^{24}}{\sigma_{flu} \times \lambda} \quad (9)$$

where:

λ = the decay constant for the selected reaction and is given by:

$$\lambda = \frac{0.693}{\tau} \quad (10)$$

τ is the reaction half-life and is given in Table 1, and Φ has units of n/cm^2. For reactions not found in Table 1, the reaction half-life may be found in the National Nuclear Data Center Nuclear Wallet Cards **(12)**.

12.2 Determine the uncertainty in the neutron fluence.

12.2.1 The dosimetry laboratory will report an uncertainty due to the measurement and counting process. Refer to this component of the fluence uncertainty as $\Delta^{flu}{}_1$. This value reflects the combination of both systematic and random components in the activity measurement process.

12.2.2 Use Table 1 to determine the cross section uncertainty at E_{flu}. If the sensors chosen are not addressed in Table 1, then use the best available dosimetry-quality cross sections. A necessary component of dosimetry-quality cross sections is the presence of covariance data. The International Reactor Dosimetry File (IRDF-90) **(15)** or the SNLRML **(16)** are recommended as sources for cross section data. Refer to this cross section component of the uncertainty as $\Delta^{flu}{}_2$.

12.2.3 The uncertainty in the neutron fluence is affected by the uncertainty in the knowledge of the neutron energy, E_{eff}. Paragraph 11.5 describes how to obtain this uncertainty in the neutron energy. Denote it as Δ^{eng}. The uncertainty in the effective neutron cross section is given by:

$$\delta\sigma_{flu} = |\Delta^{eng} \times S_{flu}| \quad (11)$$

where:

S_{flu} = the slope of the cross section as determined from the data in Fig. 6 or Table 2 or from the data in the actual cross section evaluation. Eq 9 can be used to relate this uncertainty in the effective cross section to a fluence uncertainty. Refer to this component of the fluence uncertainty as $\Delta^{flu}{}_3$. Since the decay constant has a negligible uncertainty and since uncertainty in the neutron energy does not affect the measured activity, Eq 9 indicates that if $\Delta^{flu}{}_3$ and $\delta\sigma_{flu}$ are expressed as a percentage of Φ and σ_{flu}, then $\Delta^{flu}{}_3 = \delta\sigma_{flu}$.

12.2.4 The total uncertainty in the fluence is obtained by adding in quadrature the cross section uncertainty, $\Delta^{flu}{}_2$, the measurement uncertainty, $\Delta^{flu}{}_1$, and the uncertainty component of the fluence due to the energy uncertainty, $\Delta^{flu}{}_3$, to obtain the uncertainty in the neutron energy determination. Refer to the combined uncertainty as Δ^{flu}.

12.3 *Example Calculation*—To illustrate the method, assume that the experimental procedure in Section 10 resulted in the selection of ^{93}Nb(n,2n)^{94m}Nb reaction with a measured activity of $A_{flu} = 3.63 \times 10^{-21} \pm 3.5$ % Bq/atom.

12.3.1 Using the E_{eff} = 14.5 MeV from 11.6.3, Table 2 gives a reference cross section of σ_{flu} = 0.45975 barns.

12.3.2 For the niobium reaction, Table 1 gives a half-life of τ = 10.15 d = 8.769 × 10^5 s. Thus, the decay constant is $\lambda = 7.902 \times 10^{-7}$ sec^{-1}.

12.3.3 The neutron fluence, according to Eq 9, is given by $\Phi = 3.63 \times 10^{-21} \times 10^{+24}/(0.45975 \times 7.902 \times 10^{-7}) = 9.992 \times 10^9$ n/cm^2.

12.3.4 The neutron fluence uncertainty component due to the measurement process is $\Delta^{flu}{}_1$ = 3.5 %.

12.3.5 Table 1 gives a cross section uncertainty for the niobium reaction near E_{eff} of 1.5 %. This directly translates into the neutron fluence uncertainty component due to the knowledge of the cross section, or $\Delta^{flu}{}_2$ = 1.5 %.

12.3.6 From 11.6.9 the neutron energy uncertainty is Δ^{eng} = 0.0856 MeV.

12.3.7 From Table 2, the slope of the niobium cross section near 14 MeV is S_{flu} = (0.45958 − 0.45978)/(14.75 − 14.25) = -4.0×10^{-4} b/MeV.

12.3.8 The uncertainty in the cross section due to the uncertainty in the neutron energy is $\delta\sigma_{flu} = |0.0856(-4.0 \times 10^{-4})| = 3.424 \times 10^{-5}$ b. This corresponds to a cross section uncertainty of 7.448×10^{-3} %. From 12.2.3 and Eq 7, $\Delta^{flu}{}_3 = 7.448 \times 10^{-3}$ %.

12.3.9 The total RMS value for the neutron fluence uncertainty is Δ^{flu} = sqrt(3.5 %^{2} + 1.5 %^{2} + 7.448×10^{-3} %^{2}) = 3.8 %.

13. Report

13.1 When a 14-MeV facility is characterized, a report shall be prepared that summarizes the techniques used. This report shall, at a minimum, include the following data:

13.1.1 The date and time of the characterization, the name of the primary experimenter, and all settings on the neutron generator that are required to reproduce the irradiation. The settings shall include such quantities as beam current, electrode voltage, target characteristics, and irradiation time.

13.1.2 The reactions selected for determining the neutron energy. If only a neutron fluence is determined, the report will state what neutron energy was assumed and provide a reference or rationale for the selection of this energy.

13.1.3 The reaction used to determine the neutron fluence.

13.1.4 The cross section evaluations used to characterize the reactions used.

13.1.5 If a reaction half-life was not taken from Table 1 or

Ref **(11)**, then the selected half-life and the reference will be stated. References **(19)** and **(20)** are good easily accessible compendia of nuclear data for a wide range of dosimetry reactions.

13.1.6 The dosimetry reports for all measured activities including a statement on measurement uncertainties.

13.1.7 A summary of characterized quantities including E_{eff}, Δ^{eng}, Φ, and Δ^{flu}.

13.1.8 A breakdown in the components of the uncertainties including $\Delta^{eng}{}_1$, $\Delta^{eng}{}_2$, $\Delta^{flu}{}_1$, $\Delta^{flu}{}_2$, and $\Delta^{flu}{}_3$.

13.2 Any facility characterization that is used to support facility brochures or irradiations for external customers shall be placed in a facility quality assurance file and retained for a period of at least the greater of:

13.2.1 Five years after the characterization, or

13.2.2 One year after the facility provided or referenced the document to any user or auditing agency.

14. Precision and Bias

14.1 The bias in the average neutron energy is determined primarily by the bias of the neutron interaction cross section data and only secondarily by the activity measurements if proper analytical gamma ray counting procedures are followed. Paragraph 11.5 provides a detailed methodology for calculating the precision of the average neutron energy. Table 4 provides typical uncertainties that can be achieved by utilizing this test method.

NOTE 1—Measurement uncertainty is described by a precision and bias statement in this test method. Another acceptable approach is to use Type A and B uncertainty components (see ISO "Guide to the Expression of Uncertainty in Measurement" and NIST Technical Note 1297). This Type A/B uncertainty specification is now used in International Organization for Standardization (ISO) standards and this approach can be expected to play a more prominent role in future uncertainty analyses.

14.2 The bias in the neutron fluence is determined primarily by the bias of the neutron interaction cross section data. The precision in the neutron fluence is determined primarily by the activity measurements. Paragraph 12.2 provides a detailed methodology for calculating the precision and bias of the neutron fluence. If the ^{93}Nb(n,2n)^{92m}Nb cross section is used as the monitor reaction, fluence uncertainties of about 4 % are typical. The spread in fluence values obtained by using a variety of dosimetry-quality monitor reactions is about 5 %.

15. Keywords

15.1 14-MeV; DT; neutron activation; neutron generator; neutron metrology

REFERENCES

(**1**) Liskien, H., and Paulsen, A., "Neutron Production Cross Sections and Energies for the Reactions T(p,n)^{3}He, D(d,n)^{3}He, and T(d,n)^{4}He," *Nuclear Data Tables*, Vol 11, 1973, pp. 569–619.

(**2**) Csikai, J., *CRC Handbook of Fast Neutron Generators*, Vol 1, CRC Press, Inc., 1987.

(**3**) Pavlik, A., and Winkler, G., *Calculation of the Energy Spread and Average Neutron Energy of 14 MeV Neutrons Produced Via the T(d,n)4He Reaction in Solid TiT Targets*, INDC(AVS)-011/LI, IAEA, Vienna, 1986.

(**4**) Raics, P., *Investigation of the ^{238}U(n,2n) Reaction Around 14 MeV and Its Application for the Determination of ^{238}U/ ^{235}U Isotopic Ratio*, Thesis, Kossuth Lajos University, Debrecen, Hungary, 1978 (in Hungarian).

(**5**) Csikai, J., Lantos, Z., and Buczko, M., "Investigations on the Properties of D + D and D + T Neutron Sources," IAEA Advisory Group on Properties of Neutron Sources, Leningrad, June 9–13, 1986.

(**6**) *Neutron Sources For Basic Physics and Applications, A Nuclear Energy Agency Nuclear Data Committee (OECD) Series Neutron Physics and Nuclear Data in Science and Technology*, Vol 2, A. Michaudon, S. Cierjacks, R. E. Chrien, eds., Pergamon Press, 1983.

(**7**) Brolley, J. E., Jr., and Fowler, J. L., "Monoenergetic Neutron Sources: Reactions with Light Nuclei," in *Fast Neutron Physics, Part I: Techniques*, J. B. Marion and J. L. Fowler, eds., Interscience Publishers, Inc., New York, 1960, p. 74.

(**8**) Barrall, R. C., Silbergeld, M., and Gardner, D. G., *A Method For Estimating Neutron Flux Density, Fluence, and Average Energy of Neutrons From T(d,n)He4 Reaction*, report SUHO-69-2, Stanford University, Stanford, CA, January 1969.

(**9**) *ENDF-201, ENDF/B-VI Summary Documentation*, edited by P. F. Rose, Brookhaven National Laboratory Report BNL-NCS-1741, 4th Edition, October 1991.

(**10**) Griffin, P. J., Kelly, J. G., and Luera, T. F., "Effect of ENDF/B-VI Cross Sections on Neutron Dosimetry," *Proceedings of the Seventh ASTM-Euratom Symposium on Reactor Dosimetry*, Strassbourg, France, August 27–31, 1990, pp. 669–675.

(**11**) Evaluated Nuclear Structure Data File (ENSDF), a computer file of evaluated nuclear structure and radioactive decay data, which is maintained by the National Nuclear Data Center (NNDC), Brookhaven National Laboratory (BNL), on behalf of the International Network for Nuclear Structure Data Evaluation, which functions under the auspices of the Nuclear Data Section of the International Atomic Energy Agency (IAEA). The URL is http;// www.nndc.bnl.gov/nndc/ensdf. The data quoted here comes from the database as of January 1, 2002.

(**12**) *Nuclear Wallet Cards*, compiled by J. K. Tuli, National Nuclear Data Center, January 2000.

(**13**) Holden, N. E., "Review of Thermal Cross Section and Isotopic Composition of the Elements," BNL-NCS-42224, March 1989.

(**14**) Lemmel, H. D., *X-ray and Gamma-ray Standards for Detector Calibrations*, International Atomic Energy Agency, IAEA-TECDOC-619, September 1991.

(**15**) *International Reactor Dosimetry File (IRDF-90)*, assembled by N. P. Kocherov et al., International Atomic Energy Agency, Nuclear Data Section, IAEA-NDS-141 Rev. 2, October 1993.

(**16**) Griffin, P. J., *SNL RML Recommended Dosimetry Cross Section Compendium*, Sandia National Laboratories, Albuquerque, NM, SAND92-0094, November, 1993.

(**17**) Lewis, V. E., "International Intercomparison of d + T Neutron Fluence and Energy Using Niobium and Zirconium Activation," *Metrologia*, Vol 20, 1984, pp. 49–53.

(**18**) Lewis, V. E., and Zieba, K. J., "A Transfer Standard for d + T Neutron Fluence and Energy," *Nuclear Instruments and Methods*, Vol 174, 1980, pp. 141–144.

(**19**) Browne, E., and Firestone, R. B., *Table of Radioactive Isotopes*, edited by V. S. Shirley, John Wiley & Sons, New York, 1986.

(**20**) Zijp, W. L., and Baard, J. H., *Nuclear Data Guide for Reactor Neutron Metrology, Part 1, Activation Reactions* (1979 Edition), Report ECN-70, Netherlands Energy Research Foundation ECN, Petten, August 1979. Also issued as report EUR-7164EN, Luxembourg, 1981.

(**21**) ZDrosg, M., "DROSG-2000: Neutron Source Reaction," International Atomic Energy Agency, Report IAEA-NDS-87, Revision 7, January 2002. The DROSG-2000 code distributed by the International Atomic Energry Agency and available from the web at the URL http://www-nds.iaea.or.at/ndspub/libraries/drosg2000.